applied sciences

MDPI

Article

Characterization in Dynamic Load Environment of COTS Synthetic Sapphire Bearings for Application in Magnetic Suspension in Space

Giovanni Ottavio Delle Monache [1,*], Maria Elisa Tata [2], Girolamo Costanza [2] and Claudia Cavalieri [2]

[1] INFN LNF, 00044 Frascati, Italy
[2] Industrial Engineering Department, University of Rome Tor Vergata, 00133 Rome, Italy; elisa.tata@uniroma2.it (M.E.T.); costanza@ing.uniroma2.it (G.C.); clacavalieri16@gmail.com (C.C.)
* Correspondence: giovanni.dellemonache@lnf.infn.it; Tel.: +39-06-94032544

Abstract: The present research investigates the application of a cardan suspension making use of permanent magnet (PM) bearings employed to obtain high reliable/low-cost solutions for the permanent alignment of directional payloads such as laser reflectors for the Next Generation Lunar Retroreflector (NGLR) experiment or antennas to be deployed on the moon's surface. According to Earnshaw's Theorem, it is not possible to fully stabilize an object using only a stationary magnetic field. It is also necessary to provide axial control of the shaft since the PM bearings support the radial load but, they produce an unstable axial force when losing alignment between the stator and rotor magnets stack. In this work, the use of commercial off-the-shelf (COTS) sapphire as axial bearings in the cardan suspension has been investigated by testing their behavior in response to some of the dynamic loads experienced during the qualification tests for space missions. The work is innovative in the sense that COTS sapphire assembly has never been investigated for space mission qualification. As Artemis mission loads have not been yet provided for NGLR, test loads for this study are those used for the proto-qualification of the INFN INRRI payload for the ESA ExoMars EDM mission. Tests showed that, along the x and y directions, no damages were produced on the sapphire, while, unfortunately, on the z direction both sapphires were badly damaged at nominal loads.

Keywords: magnetic suspension; jewel bearings; synthetic sapphire; alignment by gravity; dynamic loads; COTS

Citation: Delle Monache, G.O.; Tata, M.E.; Costanza, G.; Cavalieri, C. Characterization in Dynamic Load Environment of COTS Synthetic Sapphire Bearings for Application in Magnetic Suspension in Space. *Appl. Sci.* **2021**, *11*, 9027. https://doi.org/10.3390/app11199027

Academic Editor: Theodore E. Matikas

Received: 29 July 2021
Accepted: 24 September 2021
Published: 28 September 2021

1. Introduction

NASA has selected 12 new science and technology payloads, useful for the study of the Moon and to explore more of its surface as part of the Agency's Artemis lunar program [1,2]. These investigations and demonstrations will help the Agency to send astronauts to the Moon by 2024 as a way to prepare to send humans to Mars for the first time. The selected investigations will go to the Moon on future flights through NASA's Commercial Lunar Payloads Service (CLPS) projects [3]. Many of the new selections incorporate existing hardware such as parts or models designed for missions that have already flown [4]. Seven of the new selections are focused on answering questions in planetary science or heliophysics while five demonstrate new technologies. One of these 12 payloads is a new class of Lunar Laser Ranging (LLR) experiment recently investigated by international Space Agencies, named NGLR, a new concept of Cube Corner Retroreflector (CCR) to be deployed on the moon's surface. The NGLR experiment is basically a single CCR whose diameter is 100 mm that must be pointed from the Moon toward the mean Earth direction. The experiment is aimed to be integrated on a lander deck, and no robotic arm is provided for its deployment.

A simplified pointing system for the CCR could make use of a mechanism formed by a passive cardan magnetic suspension, able to compensate for the misalignment due to the

slope of the landing site that can be consistent [5], dedicated to the alignment of the CCR toward the mean Earth direction. PM bearings, providing radial trust, that are embedded in the cardan suspension for alignment by gravity of the elevation and polarization angle of the device, represent a preferred option in order to deal with the short life demonstrated by Apollo's missions' mechanisms, due to the electrostatic charged nature of Moon dust and the continuous stream of solar wind ionized particles sweeping the regolith [6,7].

Such a system can be applied to any devices in needs of permanent pointing from Moon to Earth such as telemetry antennas. With reference to a commercially available pointing mechanism, which can be complex and expensive [8], the solution does not require actuators, representing an important improvement in terms of the mass, cost and reliability of the alignment system; regarding elevation and polarization angles, it is a passive system without the provision of electrical power by the lander.

A sketch of the NGLR experiment cardan suspension layout is illustrated in Figure 1.

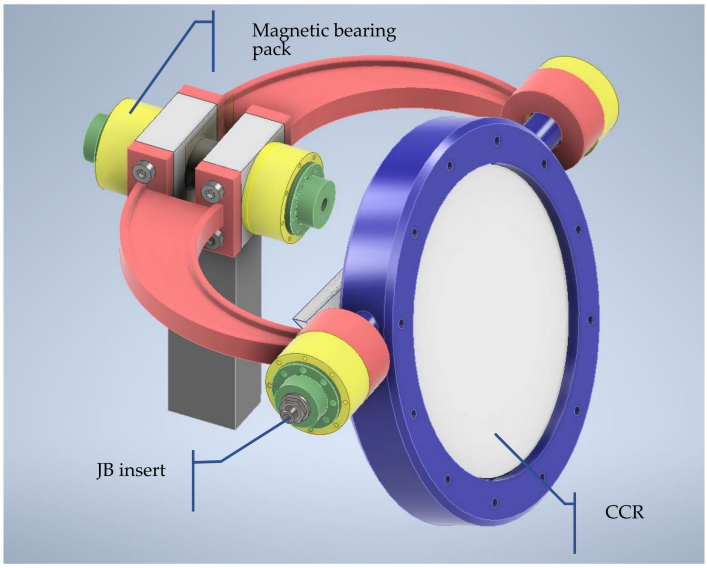

Figure 1. Sketch of the NGLR experiment cardan suspension layout.

According to Earnshaw's Theorem, it is not possible to fully stabilize an object using only a stationary magnetic field [9–11]. It is necessary to also provide axial control of the shaft since the PM bearings support the radial load, but they produce an unstable axial force when losing alignment between the stator and rotor magnets stack. The axial phasing between the rotor and the stator magnets must be accurately maintained in order to maximize the radial trust performances of the bearing. This mechanical phasing is opposed by the axial force between the stacks, which generates and tends to increase with the loss of relative nominal alignment [12]. For this reason, axial load bearings must be provided in the system design. A possible solution for stabilizing magnetic suspension in space applications considers the use of the so-called jewel bearings (JBs) where an element, normally a plate when only axial capability is required, made of synthetic sapphire [13], is axially engaged with a metal spindle. The main goal of this work is to report about the preliminary tests of COTS JB, available by Swiss Jewel Company, engaged with different material spindles. The sapphires have been subjected to the vibrational loads typical of a space mission. At the end of the tests and analysis of the results a strategy on materials and design has been developed.

2. Materials and Methods

COTS synthetic sapphire axial bearings have been subjected to dynamic tests. In detail, the tested bearings are the ES-40 models provided by Swiss Jewel. An endstone, which is a sapphire disc, is mounted on a housing that terminates with an adjusting screw,

as evidenced in Figure 1. The sapphire has a diameter of 0.187″ and a height of 0.035″ . The housing is made of 300 Series stainless steel. The endstone of the bearings is shown in Figure 2, while a picture of the bearings is reported in Figure 3.

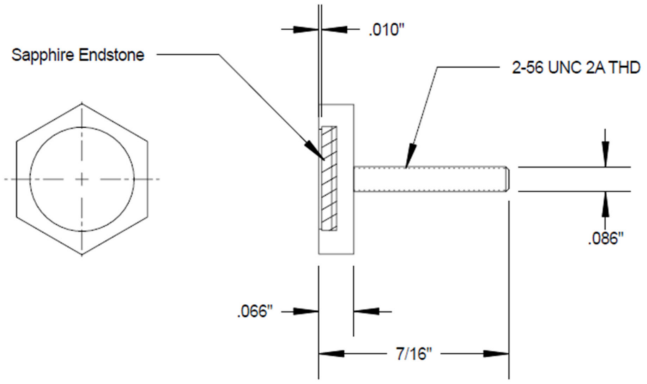

Figure 2. Endstone assembly.

Figure 3. ES-40 Bearings by Swiss Jewel.

The synthetic sapphire is a single Al_2O_3 crystal and, therefore, it exhibits alumina's chemical properties combined with mechanical properties typical of monocrystalline ceramic materials. It shows an excellent corrosion resistance and can be produced with accurate surface finishing. A preliminary hardness measurement revealed a Vickers microhardness of 2060 HV. A roughness measurement has also been conducted and the observed profile is reported in Figure 4. The measured surface roughness Ra is 0.061 +/− 0.015 µm.

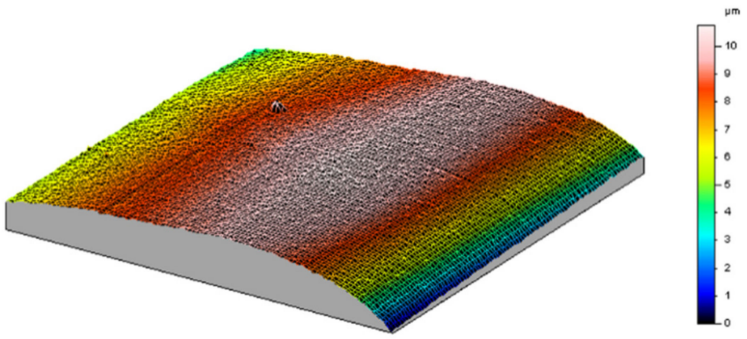

Figure 4. Surface roughness profile.

In order to allow the fastening of the test item to the shaker armature, and to properly reproduce the loads to which the bearings are subjected, a test hardware was designed. This fixture was composed of:

- an AA6081 slab used to fix the system to the shaker;
- an AISI 316 mass that reproduces the actual mass that will be aligned by means of the magnetic suspension;
- two sets of spindles, one in AA 6081 and one in AISI 316, in order to test the sapphire's response to the direct contact with two different materials having different Young's modulus;
- a frame, two flanges and a spacer realized in ASA by additive manufacturing.

The bearings have been placed in pierced thread M8 inserts. The exploded view of the system configuration for the tests conducted on *z* axis is evidenced in Figure 5.

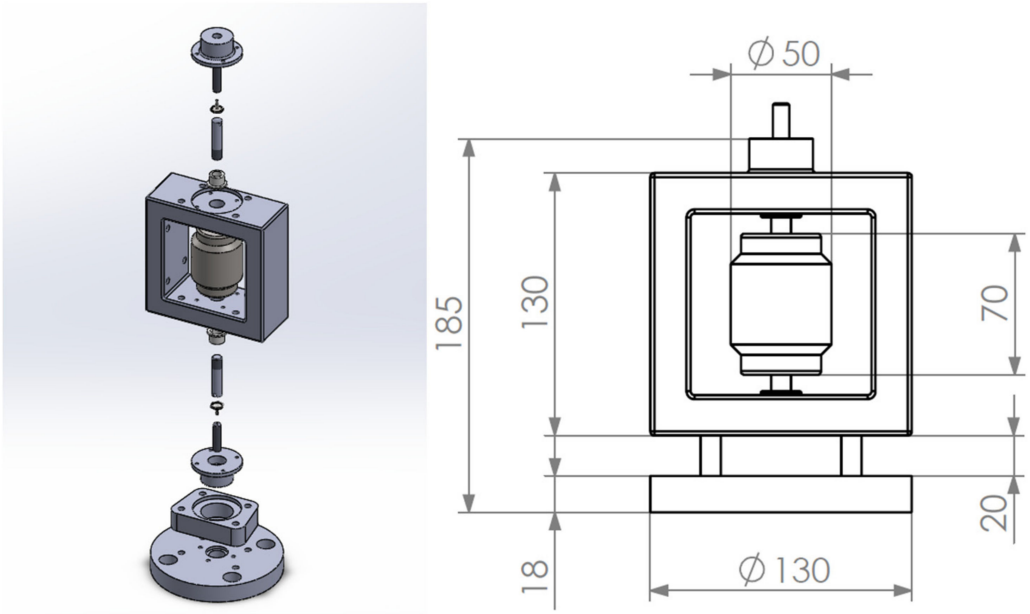

Figure 5. Layout and dimensions of the HW in the *z* axis configuration test.

The ES-40 JB has been investigated to determine its response to dynamic loads typical of qualification tests for space missions.

The vibration environment for space systems during the launch phase can be quite severe. At the end of the Critical Design Review, the integration Authority of the satellite must define the test loads that the satellite, its subsystems and payloads must survive in order for the spacecraft to be qualified for flight. For a payload integrated in a spacecraft, the loads are determined by the coupling analysis between the rocket and the spacecraft [14].

Depending on the mass, dimensions, shape and location of the item to be tested, the vibration environment can be represented by a subset of different dynamic loads that includes random vibration, sine vibration and transient or shock testing [15]. If the dimensions and the mass of the subsystem are such that the inertial loads are not negligible, the quasi static load test must be included in the list.

It is quite common that for a payload of small dimensions and mass, the envelope of the random vibration loads does include all of the vibration environment.

The vibration test system used for this purpose is a standard in the field, manufactured by Sentek Dynamics L1024M-PA115 Vibration Test System. The bearings have been tested with the loads derived by INFN INRRI experiment [16] represented by a random vibration whose test profile is shown in Figure 6. Each random test was preceded and followed by a low level sine swept test for resonance search purpose.

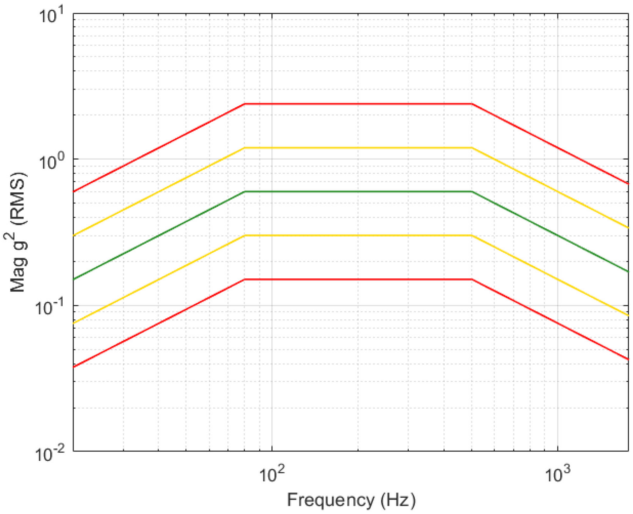

Figure 6. Random test profile.

3. Results

3.1. Preliminary Tests

After calibrating the measure and control accelerometers, a first test was carried out to make sure that the ASA structure maintained its integrity when solicitated with the test loads. No bearings were inserted in this phase, and the AISI 316 spindles were protected with Aluminum tape and brought into contact with two M8 thread inserts, wrapped in Aluminum tape. The structure underwent a random test and showed no sign of failure.

Thus, a second preliminary test was conducted with a couple of JBs and the AISI 316 spindles, to determine whether the loads on the *x* and *y* axis could damage the sapphire. The system was tested on these axes with reduced sine swept curves and a random curve, having the profile shown in Figure 6 but with a time duration of 90 s instead of 6 min. Since the bearings were not damaged, it was possible to conclude that the loads along the *x* and *y* axis (both orthogonal to the shaker's axis) could not alter their structural integrity. Therefore, it was decided not to remove the bearings after testing a single axis, but instead to check the tightening torques of both the thread inserts in which the JBs were inserted, and the M3 screws that joined the flanges and the frame, using a torque wrench.

3.2. AA 6081 Spindles

A second couple of Jewel Bearings was tested while in direct contact with the two AA 6081 spindles. Figures 7–9 show the traces of both the control and measure accelerometers, with reference to the sine swept tests conducted on each axis before and after the random tests.

After the tests along the *x* axis, the torque wrench highlighted no variation in the tightening torques. The resonance frequencies were not altered before and after the random test.

Although a shift in the resonance frequencies is visible, the tightening torque was not altered. The frequency shift has been related to the possible yield of the ASA structure. ASA has a yield stress of 27–29 MPa, which is very low if compared to AISI 316 (200 MPa) or AA 608 (145 MPa), and the additive process could sometimes not guarantee effective adhesion between ASA layers, thus reducing the nominal yield/ultimate stress.

Due to an excessive response from the system, the sine swept tests along the *z* axis were carried on with different target accelerations. Both the JBs showed damages, exhibiting radial cracks which affected the whole sapphire disc thickness. This is proved by the oxidation of the endstone housing, which can be seen in Figure 10 (2× magnification).

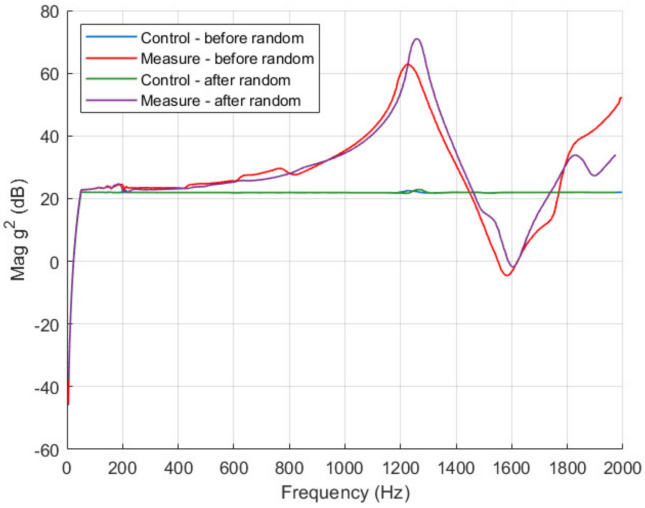

Figure 7. Resonances before and after tests on *x* axis, AA 6081 spindle.

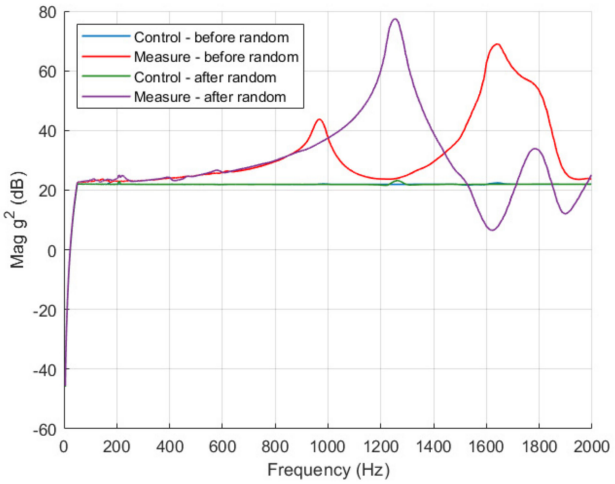

Figure 8. Resonances before and after tests on *y* axis, AA 6081 spindle.

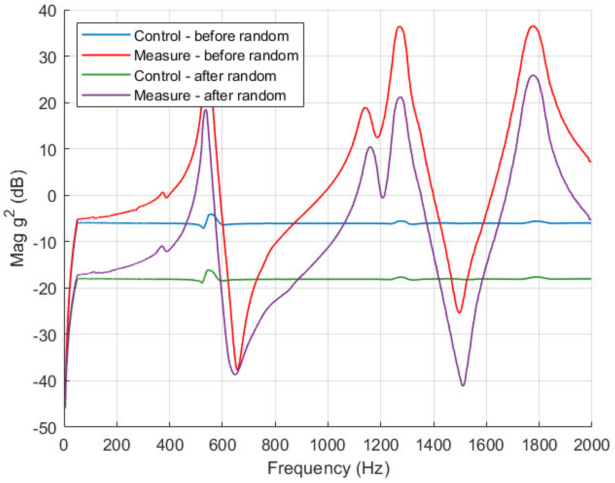

Figure 9. Resonances before and after tests on *z* axis, AA 6081 spindle.

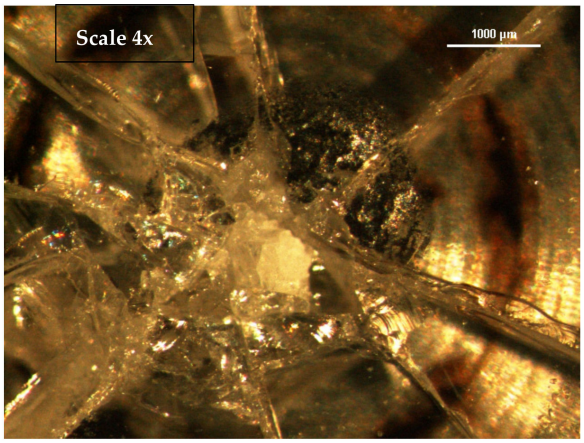

Figure 10. Lower JB on *z* axis after the test, AA6081 spindles.

The micrographs reported on Figures 10 and 11 were obtained by a stereo microscope. A partial removal of the sapphire itself is visible.

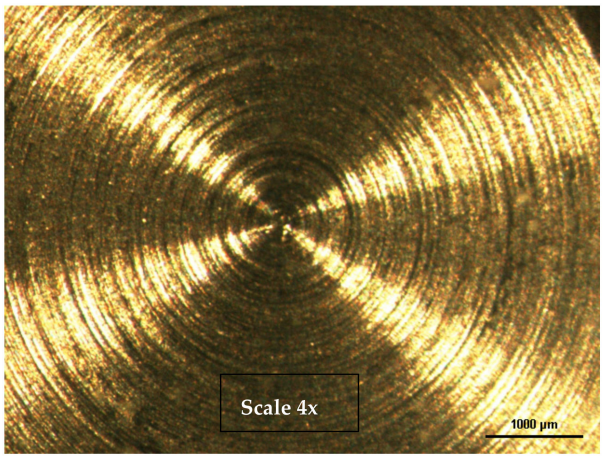

Figure 11. Lower JB on *z* axis before the test, AA 6081 spindle.

3.3. AISI 316 Spindles

Another set of JBs was tested while in direct contact with the AISI 316 spindles. Figures 12–14 show the traces of the two accelerometers during the sine swept tests conducted before and after the random tests in each axis. There was no modification either in the resonance frequencies or the tightening torques.

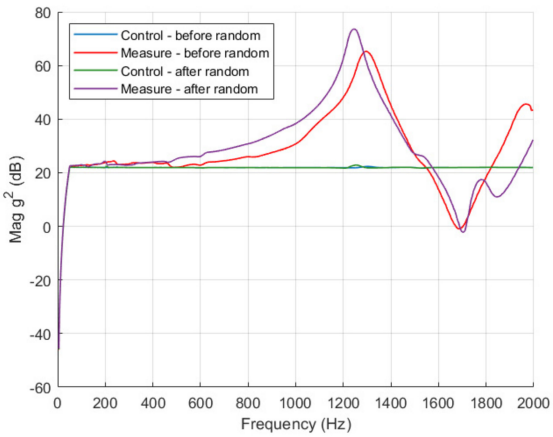

Figure 12. Resonances before and after tests on *x* axis, AISI 316 spindle.

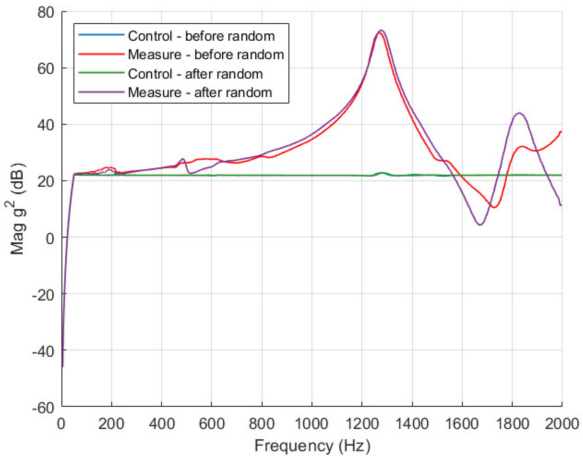

Figure 13. Resonances before and after tests on *y* axis, AISI 316 spindle.

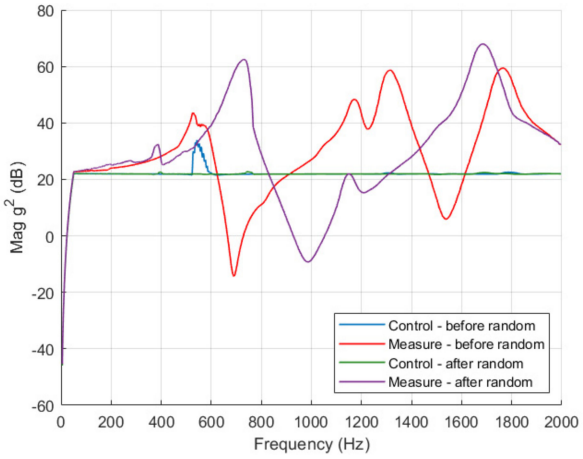

Figure 14. Resonances before and after tests on *z* axis, AISI 316 spindle.

Again, the curves reported in Figure 13 showed no major modification in the natural frequencies of the system. The torque wrench did not detect any variation in the tightening torques.

This time, the modification in the resonance frequencies was considerable and has been ascribed both to the reaching of the yield limit of the ASA structure and to a more severe damage of both JBs, which is confirmed by the micrographs (2× magnification) of the lower and most damaged bearing, shown in Figures 15 and 16.

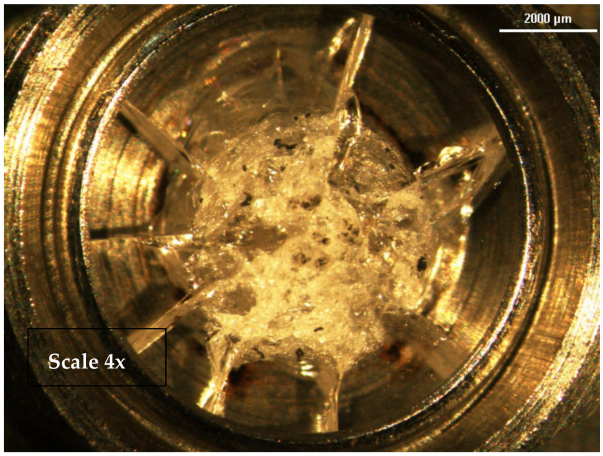

Figure 15. Lower JB on *z* axis after the test, AISI 316 spindle.

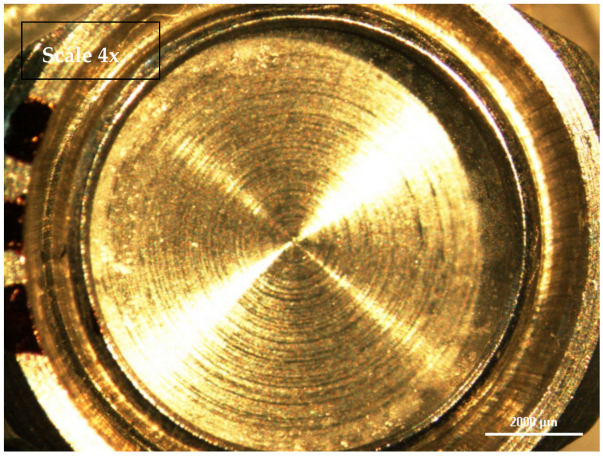

Figure 16. Lower JB on *z* axis before the test, AISI 316 spindle.

A micrography obtained with a 100× magnification is reported in Figure 17 and shows a local removal of the sapphire, affecting the whole thickness of the lower sapphire disc. Fractures could have been a consequence of impacts caused by loss of contact between the spindles and JBs during resonance. In addition, the severe damage could have been promoted by the limited thickness of the sapphire disc and the poor mechanical quality of the endstone housing. In addition, the material, of which the majority of the test hardware was made (ASA), did not allow the design of a structure with the first natural frequency beyond 2000 Hz, which represent the upper limit for a random test, usually the only one required for small payloads such as NGLR [17].

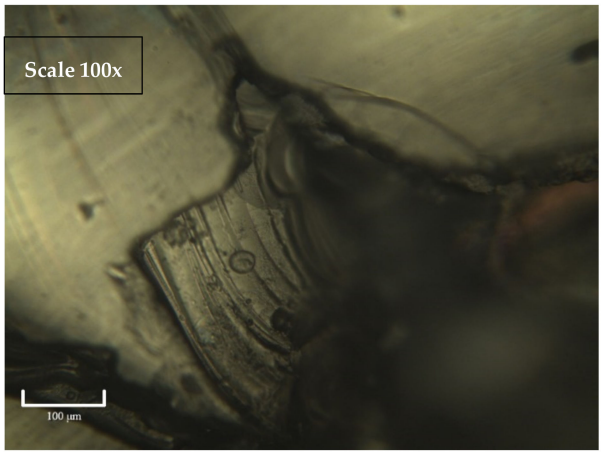

Figure 17. Partial removal of the sapphire in the lower JB.

3.4. Notching

In order to exclude that the severe damages were produced by overstressing of the system due to the stiffness of the fixture (and in our case to the lack of stiffness in the ASA frame), a simplified notching procedure [18] was carried out along the *z* axis, which proved to be the most critical one. The chosen spindles were the AISI 316 spindles. A sine swept test with a constant amplitude of 0.1 g allowed us to locate the two natural frequencies (520 Hz and 1380 Hz) within the 2000 Hz limit to be considered for the notching as shown in Figure 18.

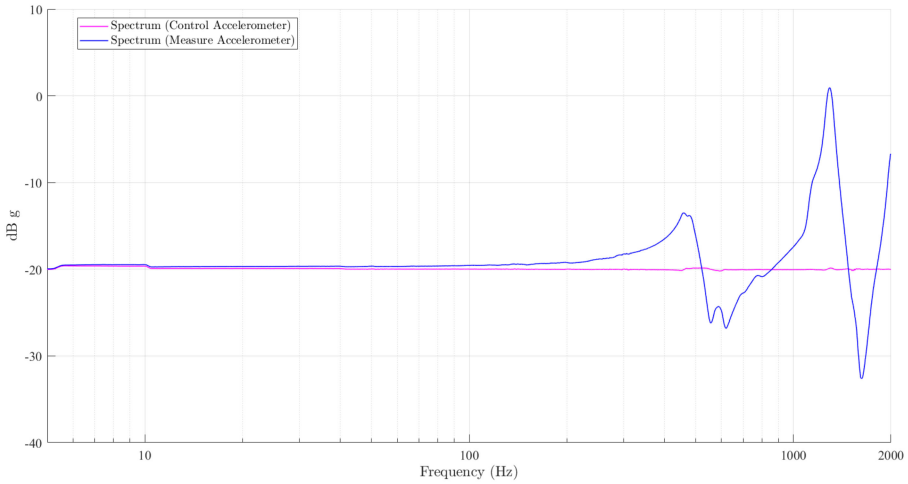

Figure 18. Natural frequencies of the system.

Then, a random test was conducted, locally reducing the load of the two orders of magnitude in correspondence with the resonance frequency. The resulting profile is shown in Figure 19. In this case the upper bearing showed no relevant damage (see Figure 20). The same cannot be said about the lower bearing (Figure 21), which was less damaged than those previously tested but still showed radial cracks extending throughout the thickness of the sapphire disc. Both micrographs were obtained with a 2× magnification.

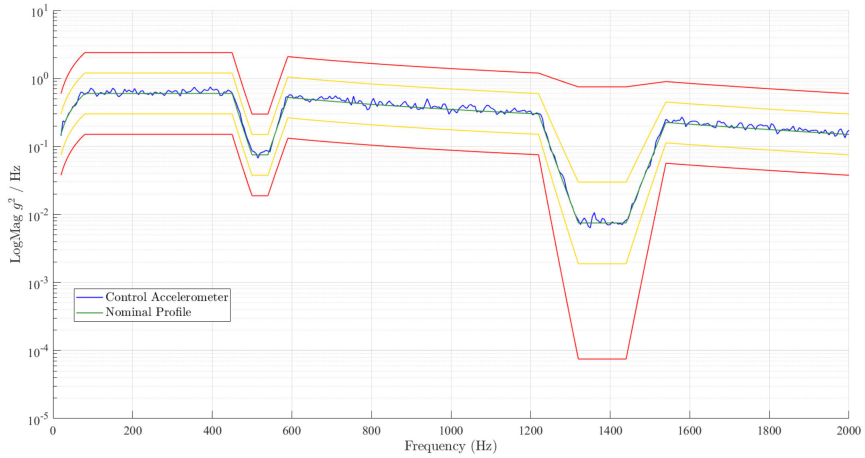

Figure 19. Notching profile.

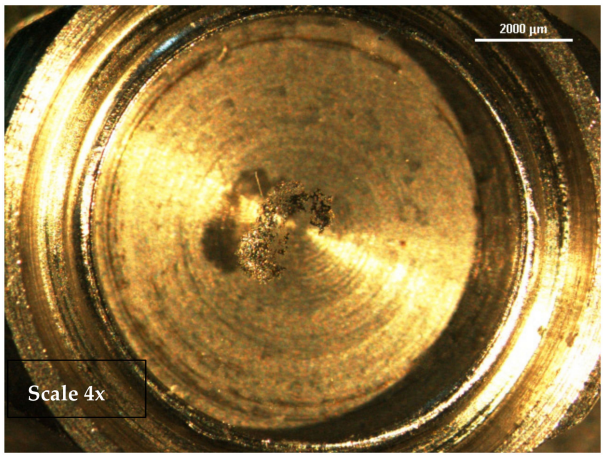

Figure 20. Upper JB after notching test.

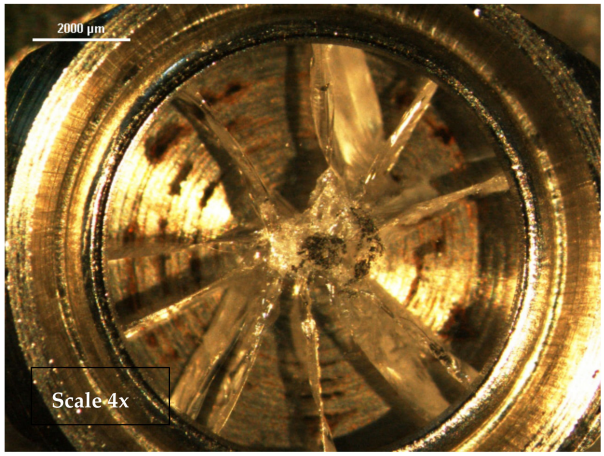

Figure 21. Lower JB after notching test.

4. Discussion

The majority of the ES-40 Jewel Bearings tested were severely damaged. Experimental results showed consistent resonance of the frame at 520 Hz and 1380 Hz. The resonance could have produced separation between the spindles and the JB and several impacts as a consequence. The damages illustrated in Figures 10, 15 and 21 at the center of the JB are consistent with those reported in [19]. However, since under certain circumstances a bearing survived the tests, the synthetic sapphire itself cannot be excluded as a possible solution for this application, especially choosing a JB having a greater thickness and tighter tolerances.

We have to consider that in single-crystal sapphires the fracture toughness shows anisotropy among the four different crystal planes [20], and this can be further investigated with the manufacturer.

In addition, the residual surface topography due to static load [21] could not lead to bearing loss. These statements provide a margin in order to develop a successful application for a flight model, considering that the mechanical design of the frame supporting the bearings must guarantee that its first resonance frequency is higher than 2000 Hz, which represents a typical requirement in payloads for space missions.

It is also appropriate to highlight that:

(1) the loads were derived by INFN INRRI experiment, and it is possible that the NGLR experiment will not be subject to the same loads;
(2) the load curves were not changed for the single axis, as is often done during qualification or verification tests;
(3) the ASA structure had a first and a second resonance frequency lower than 2000 Hz;
(4) the notching operation was simplified and not preceded by a modal analysis. Nevertheless, this has produced an important improvement in the upper JB.

Additional improvement for this application must consider the effects of surface roughness of the spindle resting on the sapphire. The mechanical layout of the magnetic bearing could produce fretting wear, which can be consistently controlled by reducing the surface roughness with laser polishing using a direct diode laser [22].

5. Conclusions

- COTS synthetic sapphire bearings have been investigated as axial bearings for a magnetic cardan suspension embedded in a passive pointing mechanism based on lunar gravity for space qualification.
- Several JB samples were tested on an HW, simulating the 1 kg estimated mass of the CCR package of the NGLR experiment, coupled with AISI 314 and AA 6081 spindles. Different load profiles have been imposed; the INFN LaRA payload for the NASA Perseverance mission, and its version with a second order manual notching.

- Tests showed that along the x and y directions no damages were produced on the sapphires. On the z direction both sapphires were badly destroyed at nominal loads. Along the same axis with dynamic load notching, the upper JB showed no damage on the surface at all.
- From the analysis, three main issues can address the failure, generated from exceeding the ultimate tensile stress in the material:
    1. Poor mechanical quality of the endstone housing, resulting in bending moment load;
    2. High stress level in the endstone due to its thickness (<1 mm);
    3. Stress amplification due to resonances of the ASA truss and cap, requiring redesigning and/or a more accurate notching analysis;

The evidence that, in some conditions, the JBs reported no damage, encourages further investigation of this solution, which is really appealing from the cost point of view. The purpose of this work is to qualify COTS JB parts as a whole for space missions. The experiment proposed can be considered as a technological demonstrator. In order to perform a quantitative analysis of the JB, an engineering model must be designed and manufactured in a way that will allow the determination of the residual starting torque in the align by gravity process of the NGLR package after the random test.

Author Contributions: All authors contributed equally to the different stages of the work. All authors have read and agreed to the published version of the manuscript.

Funding: This research received no external funding.

Institutional Review Board Statement: Not applicable.

Informed Consent Statement: Not applicable.

Acknowledgments: Authors are grateful to Fabrizio Angeloni for technical assistance in 3D printing.

Conflicts of Interest: The authors declare no conflict of interest.

References

1. Currie, D.; Dell'Agnello, S.; Delle Monache, G.O. A lunar ranging retroreflector array for the 21st century. *Acta Astron.* **2011**, *68*, 667–680. [CrossRef]
2. NASA Selects 12 New Lunar Science, Technology Investigations. Available online: https://www.nasa.gov/press-release/nasa-selects-12-new-lunar-science-technology-investigations (accessed on 30 June 2021).
3. Commercial Lunar Payload Services. Available online: https://www.nasa.gov/content/commercial-lunar-payload-services (accessed on 27 July 2021).
4. Turyshew, S.G.; Williams, J.G.; Folkner, W.M.; Gutt, G.M.; Barana, R.T.; Hein, R.C.; Somawardhana, R.P.; Lipa, J.A.; Wang, S. Corner-cube retro-reflector instrument for advanced lunar laser ranging. *Exp. Astron.* **2013**, *36*, 105–135. [CrossRef]
5. Zupp, G.A. *An Analysis and a Historical Review of the Apollo Program Lunar Module Touchdown Dynamics*; NASA SP.: Houston, TX, USA, 2013; Volume 605.
6. Heiken, G.H.; Vaniman, D.T.; French, B.M. *Lunar Sourcebook, 3.4. Dust*; Cambridge University Press: Cambridge, UK, 1991; p. 34. ISBN 0-521334446.
7. Spudis, P.D. *The Once and Future Moon*; Smithsonian Institution Press: Washington, DC, USA, 1996; pp. 89–108, ISBN 10-1560988479.
8. Merriam, E.G.; Jones, J.E.; Magleby, S.P.; Howell, L.L. Monolithic 2 DOF fully compliant space pointing mechanism. *Mech. Sci.* **2013**, *4*, 381–390. [CrossRef]
9. Earnshaw, S. On the nature of the molecular forces which regulate the constitution of the luminiferous ether. *Trans. Camb. Phil. Soc.* **1842**, *7*, 97–112.
10. Brandt, E.H. Levitation in Physics. *Science* **1989**, *243*, 349–355. [CrossRef] [PubMed]
11. Berry, M.V.; Geim, A.K. Of flying frogs and levitrons. *Eur. J. Phys.* **1997**, *18*, 307–313. [CrossRef]
12. Yonnet, J.P. Passive magnetic bearings with permanent magnets. *IEEE Trans. Magn.* **1978**, *14*, 803–805. [CrossRef]
13. Morales, W.; Fusaro, R.; Kascak, A. Permanent magnetic bearing for spacecraft applications. *Tribol. Trans.* **2008**, *46*, 460–464. [CrossRef]
14. NASA Internal Standard Load Analyses of Spacecraft and Payloads NASA-STD-5002. Revision A; 2019. Available online: https://standards.nasa.gov/standard/nasa/nasa-std-5002 (accessed on 27 July 2021).
15. Wilson, D.R. *Vibration Testing for Small Satellites*; Technical note; Boing Aerospace Corporation: Everett, WA, USA, 1989.

16. Dell'Agnello, S.; Delle Monache, G.O.; Porcelli, L.; Boni, A.; Contessa, S.; Ciocci, E.; Martini, M.; Tibuzzi, M.; Intaglietta, N.; Salvatori, L.; et al. INRRI-EDM/2016: The first laser retroreflector on the surface of Mars. *Adv. Space Res.* **2017**, *59*, 645–655. [CrossRef]
17. Calvi, A.; Aglietti, G.; Albus, J.; Bellini, M.; Burtin, D.; Cavro, E.; Dupré, J.; Fabriés, C.; Fransen, S.; Gangloff, D.; et al. *ECCS-E-HB-32-26A Spacecraft Mechanical Loads Analysis Handbook*; ESA-ESTEC: Noordwijk, The Netherlands, 2013.
18. Force Limited Vibration Testing. In *NASA Technical Handbook*; NASA-HDBK-7004B; NASA: Washington, DC, USA, 2013.
19. Luan, X.; Jiang, F.; Wang, N.; Xu, X.; Lu, X.; Qiuling, W. The mechanical response characteristics of sapphire under dynamic and quasi-static indentation loading. *Ceram. Int.* **2018**, *44*, 15208–15218. [CrossRef]
20. Huang, S.; Lin, J.; Wang, N.; Guo, B.; Jiang, F.; Wen, Q.; Lu, X. Fracture Behavior of Single-Crystal Sapphire in Different Crystal Orientations. *Crystals* **2021**, *11*, 930. [CrossRef]
21. Wang, K.; Jiang, F.; Yan, L.; Xu, X.; Wang, N.; Zha, X.; Lu, X.; Wen, Q. Study on mechanism of crack propagation of sapphire single crystals of four different orientations under impact load and static load. *Ceram. Int.* **2019**, *45*, 7359–7375. [CrossRef]
22. Ukar, E.; Lamikiz, A.; Martínez, S.; Tabernero, I.; De Lacalle, L.L. Roughness prediction on laser polished surfaces. *J. Mater. Process. Technol.* **2012**, *212*, 1305–1313. [CrossRef]